Cell Metabolism
Short Article

Apelin Stimulates Glucose Utilization in Normal and Obese Insulin-Resistant Mice

Cédric Dray,[1,2] Claude Knauf,[1,2] Danièle Daviaud,[1,2] Aurélie Waget,[1,2] Jérémie Boucher,[1,2] Marie Buléon,[1,2] Patrice D. Cani,[3] Camille Attané,[1,2] Charlotte Guigné,[1,2] Christian Carpéné,[1,2] Rémy Burcelin,[1,2] Isabelle Castan-Laurell,[1,2,*] and Philippe Valet[1,2]
[1]Institut National de la Santé et de la Recherche Médicale (INSERM), U858, Toulouse, France
[2]Université de Toulouse, UPS, Institut de Médecine Moléculaire de Rangueil (I2MR), IFR31, F-31432 Toulouse cedex 4, France
[3]Université catholique de Louvain, Unit PMNT 73/69, Brussels, Belgium
*Correspondence: isabelle.castan@inserm.fr
DOI 10.1016/j.cmet.2008.10.003

SUMMARY

Adipose tissue (AT) secretes several adipokines that influence insulin sensitivity and potentially link obesity to insulin resistance. Apelin, a peptide present in different tissues, is also secreted by adipocytes. Apelin is upregulated in obese and hyperinsulinemic humans and mice. Although a tight relation exists between the regulation of apelin and insulin, it remains largely unknown whether apelin affects whole-body glucose utilization. Herein, we show that in chow-fed mice, acute intravenous injection of apelin has a powerful glucose-lowering effect associated with enhanced glucose utilization in skeletal muscle and AT. Through in vivo and in vitro pharmacological and genetic approaches, we demonstrate the involvement of endothelial NO synthase, AMP-activated protein kinase, and Akt in apelin-stimulated glucose uptake in soleus muscle. Remarkably, in obese and insulin-resistant mice, apelin restored glucose tolerance and increased glucose utilization. Apelin could thus represent a promising target in the management of insulin resistance.

INTRODUCTION

Adipose tissue (AT) represents a major endocrine organ producing a variety of factors (adipokines) affecting insulin sensitivity and energy balance (Rosen and Spiegelman, 2006). Excess of AT in obesity induces modifications of adipokine levels known to play major roles in modulating obesity-related disorders such as type 2 diabetes or cardiovascular diseases (Mlinar et al., 2007). Adipocytes have recently been demonstrated to synthesize and secrete apelin, a bioactive peptide (Boucher et al., 2005). Apelin is also present in other tissues and in the bloodstream. It derives from a 77 amino acid precursor, processed into several active molecular forms such as apelin-13 (Carpéné et al., 2007). Apelin is the endogenous ligand of the G protein-coupled receptor, APJ (Tatemoto et al., 1998). Apelin and APJ mRNA are widely expressed in mammal tissues and are associated with functional effects in both the central nervous system and peripheral tissues (Carpéné et al., 2007).

Different studies also pointed out an emerging role of apelin in energy metabolism. A central administration of apelin was shown to reduce food intake in rat, but contrasting effects were also reported (Carpéné et al., 2007; Valle et al., 2008). Our group showed that apelin serum levels are related to the nutritional status and parallel insulin plasma levels in mice and humans (Boucher et al., 2005; Castan-Laurell et al., 2008). Furthermore, apelin plasma concentrations are increased in obese (Heinonen et al., 2005) and type 2 diabetic subjects (Li et al., 2006) as well as in hyperinsulinemic obese mice (Boucher et al., 2005). In mice, apelin inhibited glucose-stimulated insulin secretion in pancreatic islets (Sörhede Winzell et al., 2005), suggesting a link with glucose homeostasis. Recently, a 14 day apelin treatment in mice was shown to regulate adiposity and to increase uncoupling proteins expression (Higuchi et al., 2007), accounting for a role of apelin in energy metabolism.

Since plasma apelin concentrations correlate with insulinemia, similarities between apelin and insulin functions were hypothesized. The potential role of apelin in whole-body glucose disposal in normal and insulin-resistant mice remains largely unknown. In this context, our data show that, in normal mice, acute i.v. injection of apelin has a powerful glucose-lowering effect. Apelin stimulates glucose uptake in soleus muscle by endothelial nitric oxide synthase- (eNOS), AMP-activated protein kinase- (AMPK), and Akt-dependent pathways. In obese and insulin-resistant mice, apelin also improves glucose uptake in insulin-sensitive tissues underlying a relevant role of apelin in glucose metabolism.

RESULTS

Effect of Apelin on Glycemia and Glucose Utilization

A bolus of increasing concentrations of apelin was i.v. injected in mice every 45 min, and blood glucose levels were measured (Figure 1A). When compared to vehicle, a significant reduction of glycemia was observed at each time point measured after an injection of 200 pmol/kg apelin. Higher doses decreased glycemia but failed to promote a stronger effect. At the end of the experiment, apelin induced a 25% decrease in blood glucose from 1.18 ± 0.04 g/l (time 0) to 0.89 ± 0.05 g/l (time 225 min). During a single injection of 200 pmol/kg apelin, a significant decrease of glycemia was also obtained during 60 min (not shown).

During an oral glucose tolerance test (OGTT) (Figure 1B), the amplitude of the hyperglycemic response was significantly

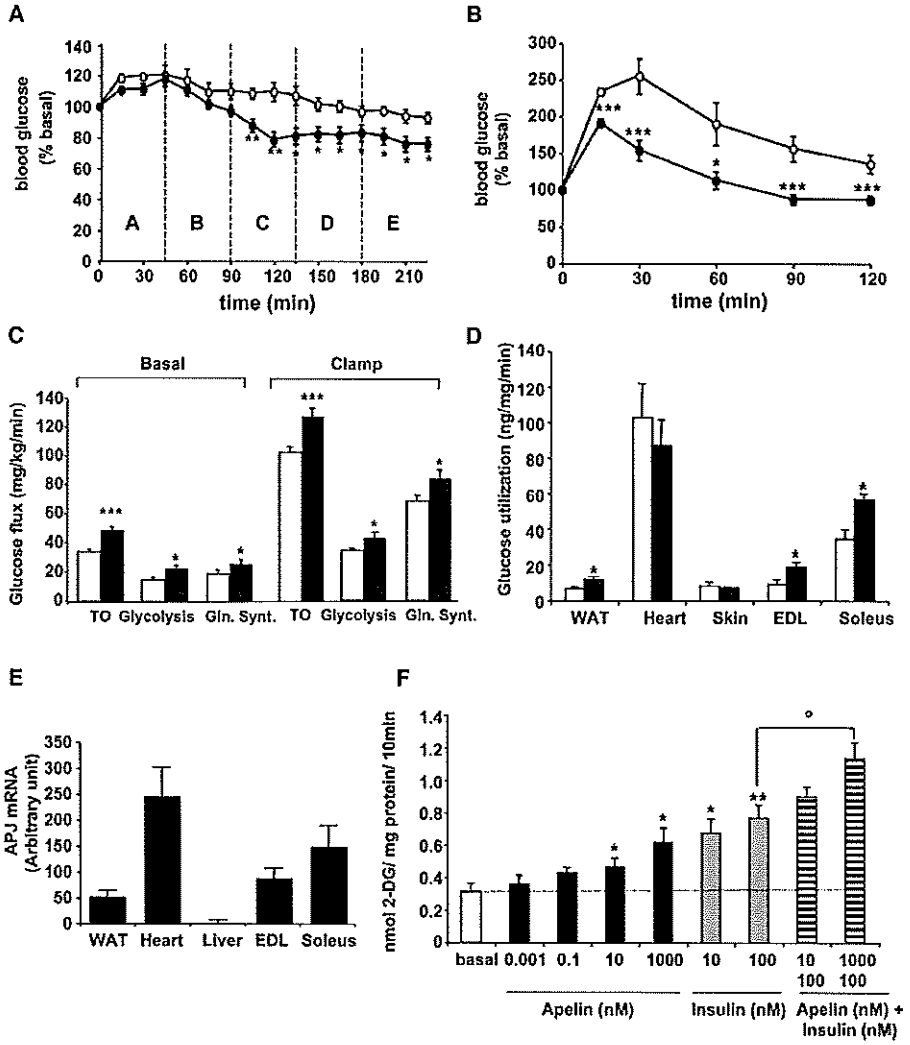

Figure 1. Apelin Decreases Glycemia and Stimulates Glucose Turnover and Utilization in WT Mice

(A) Effect of various apelin doses (A, 40 pmol/kg; B, 100 pmol/kg; C, 200 pmol/kg; D, 1000 pmol/kg; E, 2000 pmol/kg) i.v. injected every 45 min on blood glucose (black circles) compared to PBS-injected mice (white circles). Results are the mean ± SEM of five mice per group. $^{*}p < 0.05$, $^{**}p < 0.01$.

(B) OGTT in 6-hr-fasted mice i.v. injected with either PBS (white circles) or 200 pmol/kg apelin (black circles). Results are the mean ± SEM of six mice per group. $^{*}p < 0.05$, $^{***}p < 0.005$ versus control.

(C) Glucose turnover (TO) and associated glycolysis and glycogen synthesis (Gln Synt) rates in basal conditions and during an euglycemic-hyperinsulinemic clamp in control (white bars) and apelin-infused (75 pmol/kg/min) mice (black bars). The results are the mean ± SEM of five mice per group. $^{*}p < 0.05$, $^{***}p < 0.005$.

(D) Tissue glucose utilization during an euglycemic-hyperinsulinemic clamp in PBS- (white bars) and apelin-infused (75 pmol/kg/min) mice (black bars). The results are the mean ± SEM of five mice per group. $^{*}p < 0.05$ versus saline.

(E) Quantification of APJ mRNA by real-time PCR in different tissues. Results are the mean ± SEM; n = 5.

(F) Glucose uptake measured in isolated soleus muscles incubated with apelin and/or insulin at the indicated concentrations. Values are the mean ± SEM; n = 5–9. $^{*}p < 0.05$, $^{**}p < 0.01$ versus basal, $^{\circ}p < 0.05$ versus 100 nM insulin.

weaker in 200 pmol/kg apelin- compared to vehicle-injected mice. Plasma insulin levels were similar in control and apelin-injected mice (Figure S1) suggesting that, in these conditions, apelin had no effect on insulin secretion. Apelin plasma levels measured before OGTT and 15 min after glucose load were not modified (Table S1).

The influence of apelin on whole-body glucose utilization was then determined in conscious mice under basal conditions and during an euglycemic-hyperinsulinemic clamp (Figure 1C). In basal state, apelin infusion (75 pmol/kg/min) significantly increased glucose turnover (TO) and, hence, hepatic glucose production adapted to maintain euglycemia. Apelin also increased whole-body glucose TO in hyperinsulinemic conditions by stimulating whole-body glycolysis and glycogen synthesis rates. Hepatic glucose output (HGO) during clamp conditions was inhibited in the absence or presence of apelin (0.57 ± 2.1 versus 0.8 ± 3.2 mg/kg/min, respectively; n = 5). The tissues responsible for apelin-mediated increase in glucose utilization were white AT

(WAT) and skeletal muscles (soleus and extensor digitorum longus [EDL]) (Figure 1D). During the clamp, apelin infusion resulted in a physiological increase of apelinemia (maximal 2.2-fold increase) that was not influenced by hyperinsulinemia (Table S1).

In order to determine whether apelin exerts a direct effect on glucose uptake, we studied the in vitro effect of apelin in soleus muscle that express the apelin receptor (Figure 1E). Of note, APJ was not expressed in liver. Apelin stimulated glucose uptake in soleus muscle in a dose-dependent manner with a significant effect at 10 nM (Figure 1F). In addition, apelin (1 μM) was able to increase maximal insulin-stimulated glucose transport, suggesting that their effects can be additive and mediated by different mechanisms.

Apelin Signaling Involved in Muscle Glucose Uptake

Glucose transport can be stimulated via a NO-dependent pathway (Roy et al., 1998; Higaki et al., 2001). Since it has been shown that apelin activates eNOS in endothelial cells (Tatemoto et al., 2001), we first checked whether apelin was able to phosphorylate eNOS in vitro in soleus muscle. Time-course studies revealed that phosphorylation of eNOS was significantly increased at 10 min, and this effect was dose dependent (Figure 2A). In vivo, apelin also induced a significant phosphorylation of eNOS in soleus muscle (Figure 2B). In addition, the same injection of apelin did not modify the mean blood pressure and plasma NO metabolites (not shown). The importance of eNOS in apelin effect was then investigated in eNOS deficient (eNOS−/−) mice. During an euglycemic-hyperinsulinemic clamp, apelin infusion failed to increase the glucose infusion rate (GIR) (Figure 2C) and glucose utilization in WAT and muscles (Figure 2D). In vitro, 10 nM and 1 μM apelin also failed to stimulate glucose transport in soleus muscle isolated from eNOS−/− mice, whereas insulin effect was maintained (Figure 2E).

We studied AMPK as a potential upstream target of eNOS-mediated stimulation of glucose transport (Barnes and Zierath, 2005). Time-course studies in isolated soleus muscle revealed that apelin induced in parallel the phosphorylation of AMPK and acetyl-CoA carboxylase (ACC), its downstream target enzyme, at 20 until 60 min (Figure 3A). Moreover, apelin-stimulated phosphorylation of AMPK and ACC in soleus muscle was dose dependent with a significant effect at 10 nM (Figure 3A). A significant increase of AMPK and ACC phosphorylation was also observed in vivo in soleus muscle (Figure 3B). The involvement of AMPK in apelin-stimulated glucose transport was confirmed first in vitro by the use of C compound, a selective AMPK inhibitor. C Compound (20 μM) completely prevented apelin-induced AMPK phosphorylation and glucose uptake in soleus muscle (Figure 3C). Second, we performed euglycemic-hyperinsulinemic clamp studies in mice deficient in AMPK activity specifically in muscle (DN AMPK) (Mu et al., 2003) and WT mice perfused with apelin or saline. The GIR between saline-injected WT and DN-AMPK mice was similar (64.4 ± 9.3 versus 61.7 ± 9.3 mg /kg/ min; n = 3). The GIR was significantly increased in apelin-injected WT mice but not in DN-AMPK mice (88. 4 ± 2.3 versus 77.3 ± 6.8 mg /kg/ min; n = 6). Moreover, in apelin-infused DN-AMPK mice, apelin did not increase glucose utilization in muscles (EDL and soleus) compared to apelin-infused WT mice. However, apelin still increased it in WAT where AMPK is still active (Figure 3D).

In order to know whether apelin interacts with insulin signaling pathway, we studied the effect of apelin on Akt phosphorylation. In vitro time-course study in soleus muscle indicated that maximal phosphorylation by 1 μM apelin was attained at 30 min, and this effect was dose dependent (Figure 3E). In vivo, in the same conditions used to study AMPK phosphorylation, apelin also phosphorylated Akt in soleus muscle (not shown). Apelin-induced glucose transport measured in the presence of 25 μM LY294002, a specific inhibitor of PI3-kinase, was completely suppressed (Figure 3F). Finally, the relative position of the different candidates in the signaling cascade was studied (Figure 3G). In soleus muscle of DN AMPK, Akt, and eNOS were not phosphorylated by 10 nM apelin. Furthermore, LY294002 did not inhibit the phosphorylation of AMPK by10 nM apelin in soleus muscle of WT mice whereas it inhibited Akt phosphorylation. In vivo in soleus muscle of eNOS−/− mice, both AMPK and Akt were still phosphorylated 20 min after apelin injection. All together these data suggest that AMPK was upstream eNOS and Akt.

Apelin Improves In Vivo Glucose Utilization in Insulin-Resistant Mice

High fat (HF)-fed C57Bl6/J mice displaying hyperinsulinemia, hyperglycemia, and obesity (not shown) were subjected to an OGTT. HF-fed mice were largely glucose intolerant (Figure 4A). However, in apelin-injected mice, glucose tolerance was significantly improved. Fifteen minutes after oral glucose intake, insulin plasma levels were similar in control (12.15 ± 1.10 ng/ml) and in apelin-injected mice (11.94 ± 1.44 ng/ml). Apelin plasma levels were not significantly modified during the experiment (Table S1) but basal levels were increased compared to chow-fed mice (2.26 ± 0.31 versus 0.97 ± 0.09 ng/ml $p < 0.005$).

Apelin significantly increased basal glucose TO in insulin-resistant mice (Figure 4B) without affecting the mean blood glucose concentration (5.13 ± 0.69 and 5.06 ± 0.47 mM in PBS- and apelin-infused mice, respectively; n = 6). Thus apelin directly increased peripheral glucose utilization. Consequently, HGO was adapted. During euglycemic-hyperinsulinemic clamp, HGO was also inhibited in the presence of apelin (4.6 ± 3.7 versus 3.5 ± 2.2 mg/kg/min; n = 6). Insulin-resistant mice exhibited a largely blunted insulin response but apelin infusion significantly increased the GIR (Figure 4C) and glucose utilization in not only WAT, soleus, and EDL muscles but also in heart (Figure 4D).

DISCUSSION

Glucose homeostasis depends upon a balance between HGO and glucose utilization by insulin-sensitive (AT, skeletal muscle) and insulin-insensitive tissues. The present study shows, for the first time, that apelin, administered in a physiological range, improves in vivo glucose metabolism in normal and insulin-resistant HF-fed mice by increasing glucose utilization in insulin-sensitive tissues rather than HGO inhibition. In HF-fed mice, the liver becomes rapidly insulin resistant and thus HGO is not necessarily inhibited (Samuel et al., 2004). However, in our experimental conditions, the clamp procedure (high insulin levels) induced a complete suppression of HGO in both chow- and HF-fed mice as previously reported (Cani et al., 2007). By performing glucose TO measurements in a basal state in HF-fed mice, we showed that apelin directly increased peripheral glucose

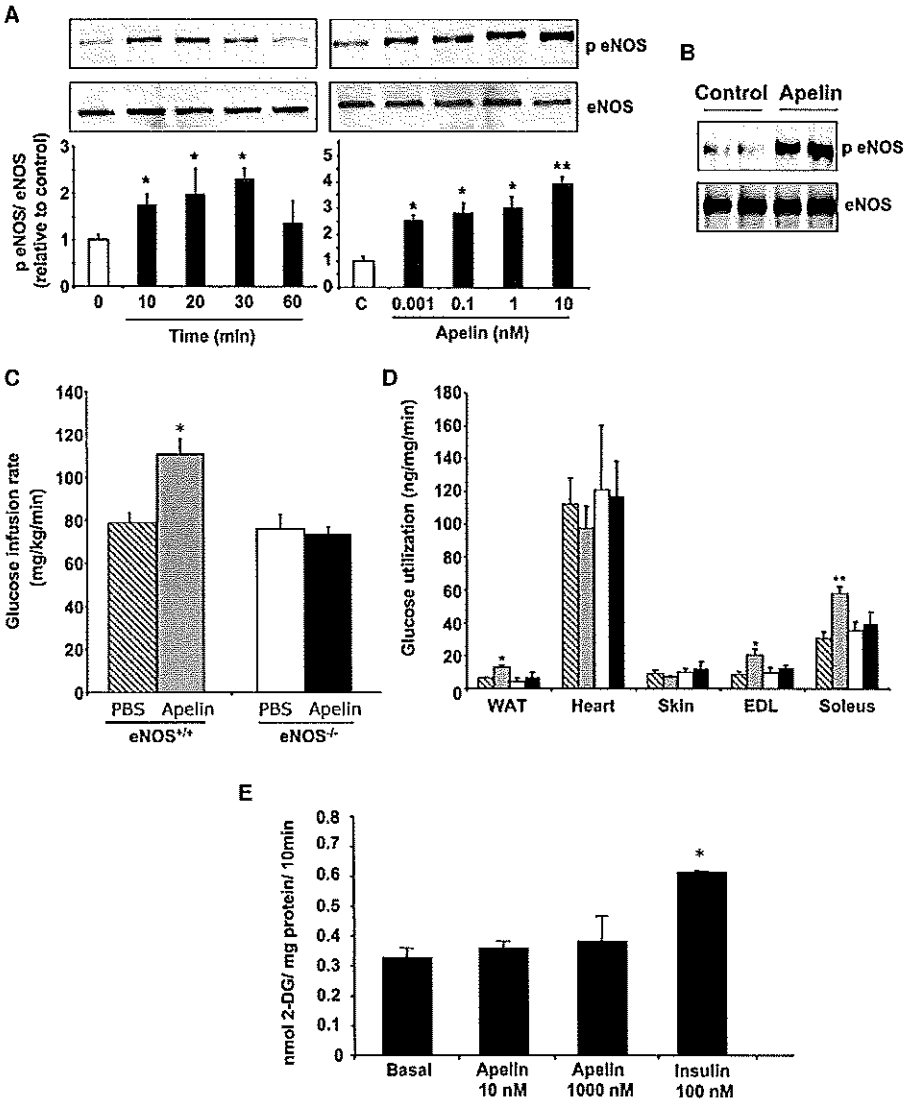

Figure 2. Apelin Effect on Glucose Utilization Is eNOS Dependent

(A) Representative blot of in vitro time-course study of eNOS phosphorylation in soleus muscles by apelin (1 μM) and dose response at the indicated apelin concentrations (incubation time with apelin: 20 min). The graph shows the quantified data; n = 3. *p < 0.05, **p < 0.01.

(B) In vivo eNOS phosphorylation in soleus muscle 20 min after an iv injection of 200 pmol/kg apelin or PBS (control) in 6-hr-fasted mice.

(C and D) Measure of GIR (C) and tissue glucose utilization (D) during an euglycemic-hyperinsulinemic clamp in apelin- (gray bars) and saline-infused (hatched bars) control mice and in apelin- (black bars) and saline-infused (white bars) eNOS−/− mice. The results are the mean ± SEM of four mice per group and per tissue. *p < 0.05, **p < 0.01.

(E) Effect of apelin and insulin on glucose uptake in soleus muscle isolated from eNOS−/− mice. The results are the mean ± SEM; n = 4. *p < 0.05 versus basal.

utilization through a most likely insulin-independent manner. Hence, HGO secondarily adapted to maintain euglycemia. The primary effect of apelin cannot target the liver during basal glucose TO experiment since there are no APJ receptors present and no change in blood glucose or insulin concentrations. However, the whole-body improvement of insulin action could have secondarily improved hepatic glucose metabolism.

In chow-fed mice, acute administration of physiological concentrations of apelin exerts a substantial glucose-lowering effect in both basal and insulin-stimulated conditions. Sörhede Winzell et al. (2005) reported that apelin had no effect on basal levels of glucose. This discrepancy could be due to the fact that, in their experiments, mice were anesthetized or that apelin-36 was used instead of apelin-13. Several endogenous fragments of physiologically active apelin have been described in tissues and blood (Carpéné et al., 2007). Apelin-13 and apelin-36 could have different effects or promote a differential desensitization pattern that may be important for their respective physiological roles as previously described (Masri et al., 2006). In the present study, no significant modification of insulin blood levels was

found between apelin- and PBS-injected mice during OGTT. Increased glucose turnover or decreased glycemia with no change of insulin plasma levels has also been described for leptin (Kamohara et al., 1997). Apelin effect might be either a direct action on glucose utilizing tissues or the result of an increased insulin sensitivity.

Hemodynamic factors have been suggested to be associated with glucose utilization. Vasodilatation is associated with enhanced insulin sensitivity, whereas vasoconstriction results in decreased glucose utilization (Juan et al., 2005). Apelin was shown to cause endothelium-dependent vasodilatation by triggering the release of NO (Tatemoto et al., 2001). The absence of apelin effect in vivo in eNOS−/− mice could result from a crosstalk between hemodynamic and direct metabolic effect of apelin on glucose uptake. The fact that apelin stimulates NO-dependent modifications of blood flow cannot be excluded as reported for insulin (Duplain et al., 2001). Alternatively, NO may act on apelin-stimulated glucose uptake, independently of its vascular action since eNOS is expressed in skeletal muscle (Kapur et al., 1997). This is further supported by the experiments performed in vitro in soleus muscle in the absence of confounding effects of blood flow. Indeed, apelin stimulates both eNOS phosphorylation and glucose uptake in soleus muscle of WT mice, and this effect is completely suppressed in eNOS−/− mice. All together these data indicate that eNOS activation is essential for apelin to exert its effect on glucose uptake.

Several studies have shown that AMPK is a possible upstream mediator of NO signaling (Fryer et al., 2000; Li et al., 2004). AMPK plays a pivotal role in the regulation of skeletal muscle glucose and fatty acid metabolism (Long and Zierath, 2006). Li et al. (2004) described the role of the NO pathway in AMPK-mediated glucose uptake in heart. Here, we provided evidence, for the first time, that apelin increases in parallel phosphorylation of AMPK and ACC in soleus skeletal muscle both in vivo and in vitro. Furthermore, AMPK is necessary to mediate the systemic action of apelin on glucose metabolism since during clamp studies in DN-AMPK mice, the apelin-stimulated glucose utilization in muscles was suppressed. However, apelin stimulates also glucose uptake by a mechanism dependent of insulin pathway. We showed, in the present study, that apelin interacts with insulin signaling at the level of PI3K/Akt. Apelin is known to phosphorylate Akt in other cell types (Carpéné et al., 2007). In addition, by combining different experiments targeting one by one the signaling molecules involved, we demonstrated that AMPK is upstream Akt and eNOS. However, we do not know whether Akt is an intermediate between AMPK and eNOS or acts in parallel to modulate the activation eNOS by apelin.

Improvement of insulin sensitivity and reduction of blood glucose levels are expected goals for the treatment of type 2 diabetes. Remarkably, we demonstrated that acute injection of apelin was able to improve glucose tolerance in HF-induced insulin-resistant mice and to increase glucose utilization in WAT, skeletal muscles, and heart. The increased glucose uptake in heart was unexpected, since it was not observed in chow-fed mice. Since glucose utilization in heart of chow-fed saline-injected mice appears maximal, the apelin effect might not be additive. Conversely, in insulin-resistant mice, apelin could ameliorate the defective glucose utilization in heart; this noticeable effect needs to be further depicted. Hence, apelin has a sustained effect on glucose utilization in insulin-resistant mice. Chronic apelin treatment will provide better insights into the tonic role of apelin in insulin-resistant mice. Higuchi et al. (2007) already observed improvement of GTT in WT mice after 14 day apelin treatment. We also found a significant amelioration of OGTT in HF-fed obese mice (not shown). Thus, apelin appears to be a promising tool in the treatment of type 2 diabetes.

In obese and hyperinsulinemic mice, we previously reported higher levels of blood apelin than in control (Boucher et al., 2005). It could be hypothesized that the high levels of circulating apelin found in obese help to delay the onset of insulin resistance. Over time, the endogenous apelin might be either insufficient or inefficient. Apelin peptides are subjected to enzymatic degradation leading to inactive forms of apelin (Carpéné et al., 2007). These inactive forms cannot be discriminated from the active ones in the assay used. Very recently, Valle et al. (2008) demonstrated that in vitro, apelin-13 was progressively converted to [Pyr1] apelin and no other breakdown products were found. Another hypothesis is that the high levels of apelin lead to apelin resistance. However, Zhong et al. (2007) showed that even if there is a depressed expression of apelin receptor in aortic rings of diabetic mice, apelin enhanced phosphorylation of eNOS and Akt. Thus, the apelin-mediated biological effects observed herein in insulin-resistant mice might be due to the added exogenous active form of apelin-13 in the bloodstream.

In conclusion, the present study reveals apelin as a new endocrine regulator of AMPK and strengthens the crosstalk between AT and skeletal muscle. The involvement of AMPK in apelin-mediated glucose uptake represents an attractive pathway that could conceivably lead to new drug target for the treatment of metabolic disorders. The contribution of apelin should yield new insights into the physiology and physiopathology of glucose and lipid metabolism.

EXPERIMENTAL PROCEDURES

Animals and Diets

Animals were handled in accordance with the principles and guidelines established by the National Institute of Medical Research. C57Bl6/J WT and eNOS−/− mice were obtained from Charles River Laboratory (l'Arbresle, France). Mice deficient in AMPK activity (DN AMPK) were kindly provided by the laboratory of Pr. Birnbaum (University of Pennsylvania Medical School; Philadelphia, USA). Mice were housed conventionally in a constant temperature (20°C–22°C) and humidity (50%–60%) animal room, with a 12/12 hr light/dark cycle and free access to food and water. Injections and experiments were performed in 13- to 15-week-old males. A group of male mice was fed a HF containing 20% protein, 35% carbohydrate, and 45% fat (SAFE; Augy, France). HF-fed mice were followed at regular with measure of body weight and blood parameters (glucose, insulin) until they were obese and insulin resistant (30–35 weeks old).

In Vivo Injection of Apelin

A catheter was indwelled into the femoral vein under anesthesia, sealed under the back skin, and glued on the top of the skull. The mice were housed individually and allowed to recover for 3–4 days. On the day of the experiment the mice were 6 hr fasted. Conscious mice were then injected with either apelin-13 or PBS. Apelin (Bachem, UK) was injected as a bolus (100 μl/2 min) for glycemia measurements.

Oral Glucose Tolerance Test

Six-hour-fasted mice were injected with apelin-13 (200 pmol/kg) or PBS 30 min before oral glucose (3 g/kg) load. Blood was collected from the tail vein at −30,

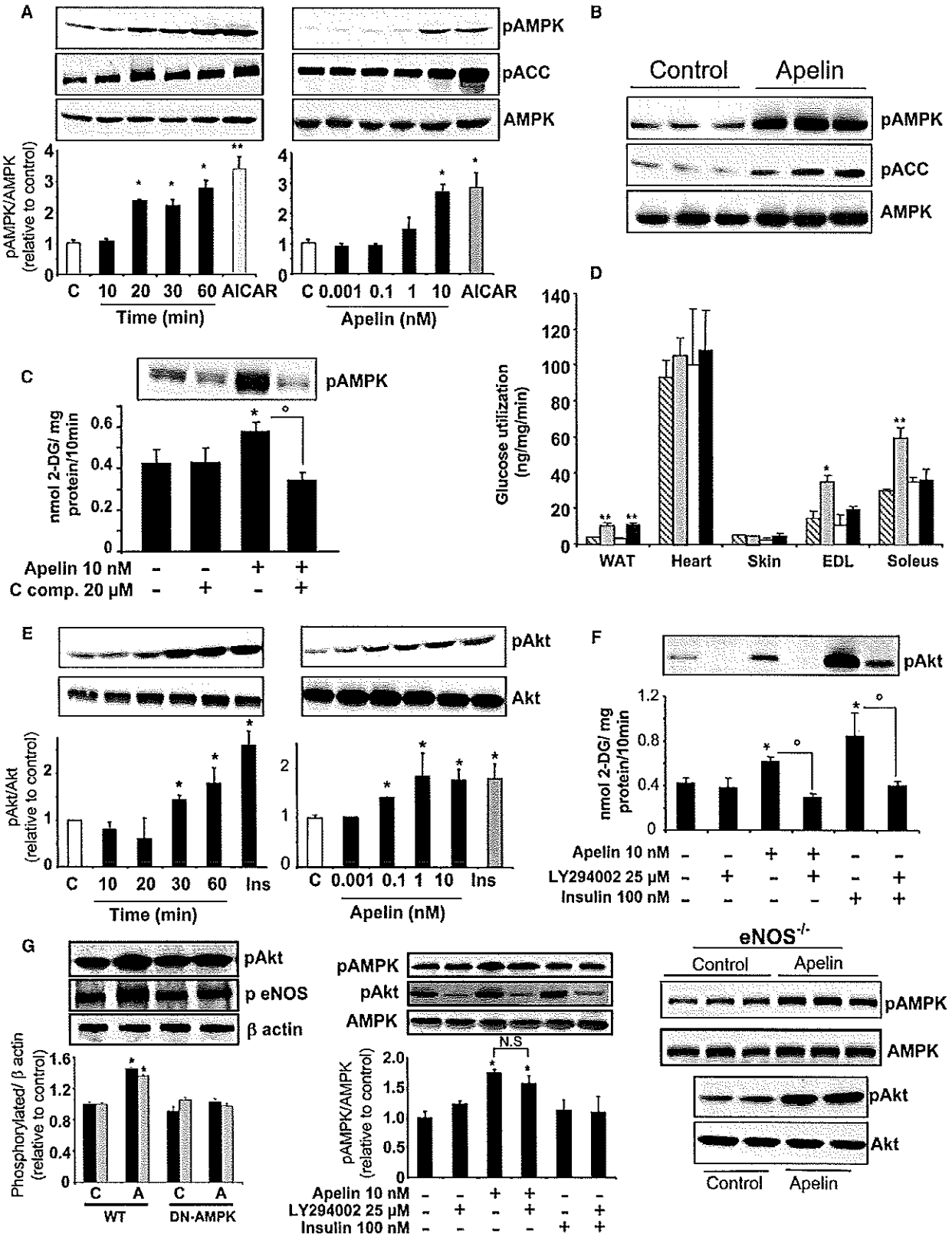
A
pAMPK
pACC
AMPK
pAMPK/AMPK (relative to control)
C 10 20 30 60 AICAR
Time (min)
C 0.001 0.1 1 10 AICAR
Apelin (nM)
B
Control
Apelin
pAMPK
pACC
AMPK
C
pAMPK
nmol 2-DG/ mg protein/10min
Apelin 10 nM
C comp. 20 μM
D
Glucose utilization (ng/mg/min)
WAT
Heart
Skin
EDL
Soleus
E
pAkt
Akt
pAkt/Akt (relative to control)
C 10 20 30 60 Ins
Time (min)
C 0.001 0.1 1 10 Ins
Apelin (nM)
F
pAkt
nmol 2-DG/ mg protein/10min
Apelin 10 nM
LY294002 25 μM
Insulin 100 nM
G
pAkt
p eNOS
β actin
Phosphorylated/ β actin (relative to control)
C A C A
WT
DN-AMPK
pAMPK
pAkt
AMPK
N.S
pAMPK/AMPK (relative to control)
Apelin 10 nM
LY294002 25 μM
Insulin 100 nM
eNOS-/-
Control
Apelin
pAMPK
AMPK
pAkt
Akt
Control
Apelin

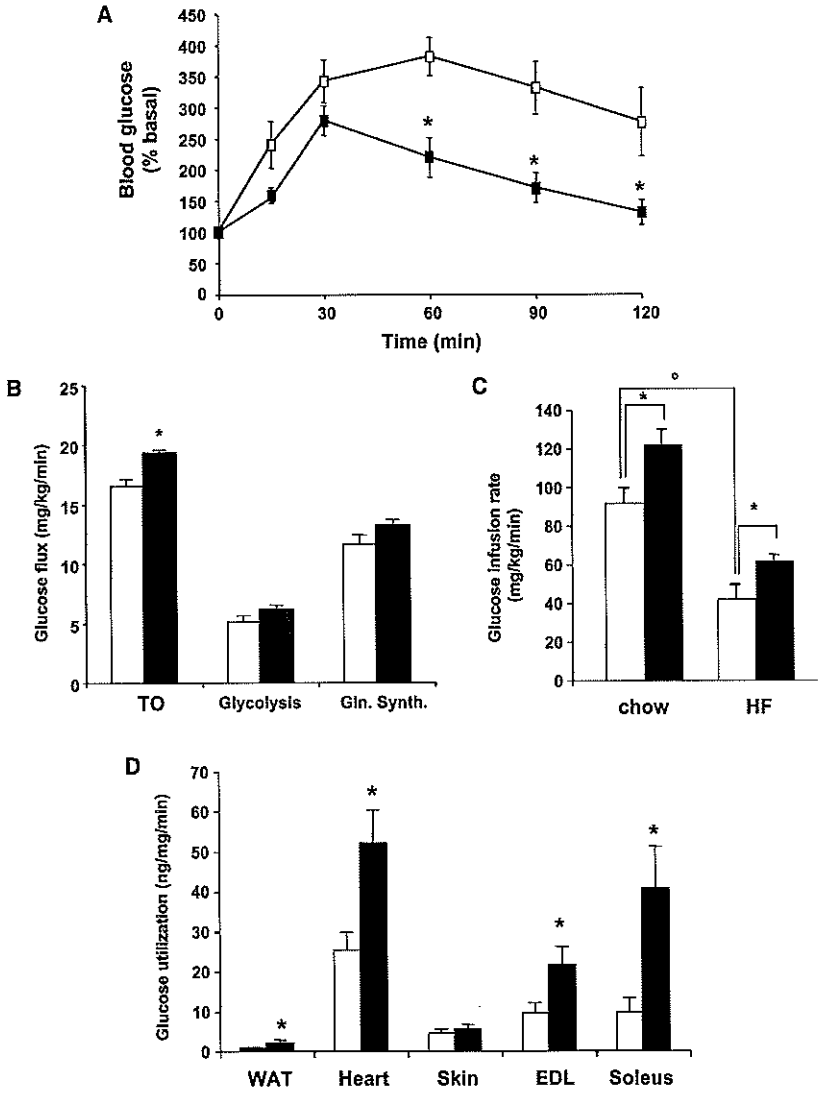

Figure 4. Apelin Improves Glucose Tolerance and Glucose Utilization in HF-Fed Insulin-Resistant Mice

(A) OGTT performed in 6-hr fasted insulin-resistant mice i.v. injected with PBS (white square) or 200 pmol/kg apelin (black squares). The results are the mean ± SEM of six mice per group. *$p < 0.05$.

(B) Basal glucose TO in control (white bars) and apelin-infused (75 pmol/kg/min) mice (black bars). The results are the mean ± SEM of six mice per group. *$p < 0.05$.

(C) GIR during an euglycemic-hyperinsulinemic clamp in chow-fed and HF-fed mice infused with saline (white bars) or apelin (75 pmol/kg/min) (black bars). The results are the mean ± SEM of six mice per group. *$p < 0.05$ versus saline °$p < 0.05$ versus chow-fed mice.

(D) Tissue glucose utilization during an euglycemic-hyperinsulinemic clamp in saline- (white bars) and apelin-infused (75 pmol/kg/min) (black bars) mice. The results are the mean ± SEM of five mice per group and per tissue. *$p < 0.05$ versus saline.

Glucose Turnover Studies

Whole-body glucose utilization rate was determined in basal and in hyperinsulinemic euglycemic conditions in 6-hr-fasted mice. In basal state, HPLC purified D-[^{3}H]-glucose (Perkin Elmer; Boston, MA) was continuously infused in the femoral vein at a rate of 10 μCi/kg/min for 3 hr. Under hyperinsulinemic conditions, insulin was infused at a rate of 18 mU/kg/min for 3 hr. Apelin-13 was continuously infused either in basal or under hyperinsulinemic conditions at a rate of 75 pmol/kg/min for 3 hr. To ensure a sufficient plasma D-[^{3}H]-glucose enrichment the tracer was infused at 30 μCi/kg/min. Plasma glucose concentrations and D-[^{3}H]-glucose-specific activity were determined in 5 μl of blood sampled as previously described (Perrin et al., 2004). The whole-body glycolytic flux was calculated from the [^3H_2O] accumulated in the plasma during the last 60 min of the infusions. The whole-body glycogen synthesis rate was calculated by subtracting the glycolytic flux from the glucose TO rate as previously described (Perrin et al., 2004).

0, 15, 30, 60, 90, and 120 min and glycemia measured with a gluco-meter (Accu-check Actine, Roche). Blood was also collected 30 min before glucose load and during OGTT for plasma insulin and apelin concentrations.

Figure 3. Involvement of AMPK and Akt in Apelin-Induced Glucose Transport in Soleus Muscle

(A) Representative blot of in vitro time-course study of AMPK and ACC phosphorylation in soleus muscles by apelin (1 μM) and dose response (incubation time with apelin: 20 min). Two millimolar 5-aminoimidazole-4-carboxamide-1-b-D-ribofuranoside (AICAR) for 1 hr was used as a positive control. The graph shows the quantified data; n = 3–4; *$p < 0.05$, **$p < 0.01$.

(B) In vivo AMPK and ACC phosphorylation in soleus muscle 20 min after an i.v. injection of 200 pmol/kg apelin or PBS (control) in 6-hr-fasted mice.

(C) Effect of 20 μM C compound on AMPK phosphorylation (top) and glucose transport (bottom) stimulated by apelin in isolated soleus muscle. Values are the mean ± SEM, n = 5. *$p < 0.05$ versus basal and °$p < 0.05$ versus apelin.

(D) Measure of tissue glucose utilization during an euglycemic-hyperinsulinemic clamp in apelin- (black bars) and saline-infused (white bars) DN-AMPK mice and in apelin- (gray bars) and saline-infused (hatched bars) WT mice. The results are the mean ± SEM of 3–6 mice per group and per tissue. *$p < 0.05$, **$p < 0.01$.

(E) Representative blot of in vitro time-course study of Akt phosphorylation in soleus muscles by apelin (1 μM) and dose response (incubation time with apelin: 30 min). Insulin (100 nM) for 1 hr in time-course study or 30 min in the dose response was used as a positive control. The graphs show the quantified data, n = 3–4. *$p < 0.05$.

(F) Effect of 25 μM LY294002 on Akt phosphorylation (top) and glucose transport (bottom) stimulated by apelin or insulin in isolated soleus muscle. Values are the mean ± SEM, n = 3–4. *$p < 0.05$ versus basal and °$p < 0.05$ versus apelin or insulin.

(G) Left: Akt and eNOS phosphorylation in isolated soleus muscle of WT and DN-AMPK mice incubated without (C) or with 10 nM apelin (A). The graph shows the quantified data n = 3 of Akt (black bars) and eNOS (gray bars). Middle: effect of 25 μM LY294002 on AMPK and Akt phosphorylation in soleus muscle of WT mice in the presence or not of 10 nM apelin or 100 nM insulin (incubation time: 30 min). The graph shows the quantified data, n = 3. *$p < 0.05$ versus control. Right: In vivo AMPK and Akt phosphorylation in soleus muscle, 20 min after an i.v. injection of 200 pmol/kg apelin or PBS (control), in 6-hr-fasted eNOS−/− mice.

In Vivo Glucose Utilization in Individual Tissues

To determine the insulin and apelin-stimulated glucose utilization in tissues, a flash of intravenous injection of 50 μCi 2-deoxy-D-[^{3}H] glucose (D-[^{3}H]-2DG) (NEN LifeScience) was performed in the femoral vein 60 min before the end of the clamp. Plasma D-[^{3}H]-2DG disappearance and glucose concentration were determined in 5 μl blood sampled from the tail vein at 0, 5, 10, 15, 20, 25, 30, 45, and 60 min after injection. Different tissues were dissected out and treated as previously described (Kamohara et al., 1997).

Glucose Transport in Soleus Muscle

Muscles were isolated and preincubated for 10 min in Krebs-Henseleit (KH) buffer, pH 7.4, containing BSA (2 mg/ml), 2 mM sodium pyruvate, and 20 mM HEPES. Muscles were then incubated for 45 min in the absence or the presence of insulin and/or apelin-13. For glucose transport, muscles were transferred in another vial containing KH medium supplemented with D-2DG (0, 1 mM) and D-[^{3}H]-2DG (0.4 μCi/ml) for 10 min. Muscles were then washed for 1 hr in ice-cold iso-osmotic NaCl solution and dissolved in 1 M NaOH during 1 hr. D-[^{3}H]-2DG 6-phosphate and D-[^{3}H]-2DG were differentially precipitated by the use of zinc sulfate (0.3 M), baryum hydroxide (0.3 M) and perchloric acid solutions (6%).

In order to determine the implication of AMPK and Akt in apelin-stimulated glucose transport, 20 μM C Compound or 25 μM LY 294002, respectively, were added during the preincubation and incubation of soleus muscle with apelin. All the incubations were carried out at 37°C under a 95% O_2: 5% CO_2 atmosphere.

Western Blots

Muscle samples were lysed (precellys 24, Ozyme France) and loaded (50 μg protein per lane) on a 10% SDS-PAGE gel and transferred to nitrocellulose membrane (Schleicher-Schuell). Membranes were blotted with anti-phospho-AMPKα-Thr172, anti-phospho-ACC-Ser79, anti-phospho-eNOS-Ser1177 or anti-phospho-Akt-Ser473 antibodies (Cell Signaling Technology; Beverly, MA). Membranes were then stripped and reprobed with specific antibodies for total proteins. Immunoreactive proteins were detected using the ECL Plus (GE Healthcare, UK) and quantified by Image Quant TL software (GE Healthcare Bio-sciences, Sweden).

Real-Time PCR

Total RNAs (1 μg) were isolated from AT using RNeasy Lipid Tissue Kits (QIAGEN, France) and from other tissues (muscle, heart, liver) using RNA STAT (AMS Technology, UK). Total RNAs were reverse transcribed using random hexamers and Superscript II reverse transcriptase (Invitrogen, UK). Real-time PCR was performed as previously described (Boucher et al., 2005). The sequences of the primers for apelin receptor were 5′-GCTGTGCCTGTCA TGGTGTT- 3′ and 5′-CACTGGATCTTGGTGCCATTT-3′.

Plasma Samples

Serum insulin and apelin concentrations were measured using an ultrasensitive mouse insulin ELISA (Mercodia; Uppsala, Sweden) and a nonselective apelin-12 EIA kit (Phoenix Pharmaceuticals; Belmont, CA), respectively.

Statistical Analysis

Data are presented as means ± SEM. Analysis of differences between groups was performed with Student's t test, and $p < 0.05$ was considered to be significant.

SUPPLEMENTAL DATA

Supplemental Data include one figure and one table and can be found online at http://www.cell.com/cellmetabolism/supplemental/S1550-4131(08)00321-5.

ACKNOWLEDGMENTS

We gratefully acknowledge the animal facilities staff and Y. Barreira (service de Zootechnie, IFR31), M. Birnbaum (HHMI, University of Pennsylvania; Philadelphia, USA) for providing DN-AMPK mice as well as J.S. Saulnier-Blache and M. Lafontan for fruitful discussions and reviewing of the manuscript.

Received: July 27, 2007
Revised: May 20, 2008
Accepted: October 8, 2008
Published: November 4, 2008

REFERENCES

Barnes, B.R., and Zierath, J.R. (2005). Role of AMP-activated protein kinase in the control of glucose homeostasis. Curr. Mol. Med. *5*, 341–348.

Boucher, J., Masri, B., Daviaud, D., Gesta, S., Guigné, C., Mazzucotelli, A., Castan-Laurell, I., Tack, I., Knibiehler, B., Carpene, C., et al. (2005). Apelin, a newly identified adipokine up-regulated by insulin and obesity. Endocrinology *146*, 1764–1771.

Cani, P.D., Amar, J., Iglesias, M.A., Poggi, M., Knauf, C., Bastelica, D., Neyrinck, A.M., Fava, F., Tuohy, K.M., Chabo, C., et al. (2007). Metabolic endotoxemia initiates obesity and insulin resistance. Diabetes *56*, 1761–1772.

Carpéné, C., Dray, C., Attané, C., Valet, P., Portillo, M.P., Churruca, I., Milagro, F.I., and Castan-Laurell, I. (2007). Expanding role for the apelin/APJ system in physiopathology. J. Physiol. Biochem. *63*, 359–373.

Castan-Laurell, I., Vitkova, M., Daviaud, D., Dray, D., Kovacikova, M., Kovacova, Z., Hejnova, J., Stich, V., and Valet, P. (2008). Effect of hypocaloric-induced weight loss in obese women on plasma apelin and adipose tissue expression of apelin and APJ. Eur. J. Endocrinol. *158*, 905–910.

Duplain, H., Burcelin, R., Sartori, C., Cook, S., Egli, M., Lepori, M., Vollenweider, P., Pedrazzini, T., Nicod, P., Thorens, B., and Scherrer, U. (2001). Insulin resistance, hyperlipidemia, and hypertension in mice lacking endothelial nitric oxide synthase. Circulation *104*, 342–345.

Fryer, L.G., Hajduch, E., Rencurel, F., Salt, I.P., Hundal, H.S., Hardie, D.G., and Carling, D. (2000). Activation of glucose transport by AMP-activated protein kinase via stimulation of nitric oxide synthase. Diabetes *49*, 1978–1985.

Heinonen, M.V., Purhonen, A.K., Miettinen, P., Paakkonen, M., Pirinen, E., Alhava, E., Akerman, K., and Herzig, K.H. (2005). Apelin, orexin-A and leptin plasma levels in morbid obesity and effect of gastric banding. Regul. Pept. *130*, 7–13.

Higaki, Y., Hirshman, M.F., Fujii, N., and Goodyear, L.J. (2001). Nitric oxide increases glucose uptake through a mechanism that is distinct from the insulin and contraction pathways in rat skeletal muscle. Diabetes *50*, 241–247.

Higuchi, K., Masaki, T., Gotoh, K., Chiba, S., Katsuragi, I., Tanaka, K., Kakuma, T., and Yoshimatsu, H. (2007). Apelin, an APJ receptor ligand, regulates body adiposity and favors the messenger ribonucleic acid expression of uncoupling proteins in mice. Endocrinology *148*, 2690–2697.

Juan, C.C., Chien, Y., Wu, L.Y., Yang, W.M., Chang, C.L., Lai, Y.H., Ho, P.H., Kwok, C.F., and Ho, L.T. (2005). Angiotensin II enhances insulin sensitivity in vitro and in vivo. Endocrinology *146*, 2246–2254.

Kamohara, S., Burcelin, R., Halaas, J.L., Friedman, J.M., and Charron, M.J. (1997). Acute stimulation of glucose metabolism in mice by leptin treatment. Nature *389*, 374–377.

Kapur, S., Bédard, S., Marcotte, B., Côté, C.H., and Marette, A. (1997). Expression of nitric oxide synthase in skeletal muscle: a novel role for nitric oxide as a modulator of insulin action. Diabetes *46*, 1691–1700.

Li, J., Hu, X., Selvakumar, P., Russell, R.R., III, Cushman, S.W., Holman, G.D., and Young, L.H. (2004). Role of the nitric oxide pathway in AMPK-mediated glucose uptake and GLUT4 translocation in heart muscle. Am. J. Physiol. Endocrinol. Metab. *287*, E834–E841.

Li, L., Yang, G., Li, Q., Tang, Y., Yang, M., Yang, H., and Li, K. (2006). Changes and relations of circulating visfatin, apelin, and resistin levels in normal, impaired glucose tolerance, and type 2 diabetic subjects. Exp. Clin. Endocrinol. Diabetes *114*, 544–548.

Long, Y.C., and Zierath, J.R. (2006). AMP-activated protein kinase signaling in metabolic regulation. J. Clin. Invest. *116*, 1776–1782.

Masri, B., Morin, N., Pedebernade, L., Knibiehler, B., and Audigier, Y. (2006). The apelin receptor is coupled to Gi1 or Gi2 protein and is differentially desensitized by apelin fragments. J. Biol. Chem. *281*, 18317–18326.

Mlinar, B., Marc, J., Janez, A., and Pfeifer, M. (2007). Molecular mechanisms of insulin resistance and associated diseases. Clin. Chim. Acta *375*, 20–35.

Mu, J., Barton, E.R., and Birnbaum, M.J. (2003). Selective suppression of AMP-activated protein kinase in skeletal muscle: update on 'lazy mice'. Biochem. Soc. Trans. *31*, 236–241.

Perrin, C., Knauf, C., and Burcelin, R. (2004). Intracerebroventricular infusion of glucose, insulin, and the adenosine monophosphate-activated kinase activator, 5-aminoimidazole-4-carboxamide-1-beta-D-ribofuranoside, controls muscle glycogen synthesis. Endocrinology *145*, 4025–4033.

Rosen, E.D., and Spiegelman, B.M. (2006). Adipocytes as regulators of energy balance and glucose homeostasis. Nature *444*, 847–853.

Roy, D., Perreault, M., and Marette, A. (1998). Insulin stimulation of glucose uptake in skeletal muscles and adipose tissues in vivo is NO dependent. Am. J. Physiol. *274*, E692–E699.

Samuel, V.T., Liu, Z.X., Qu, X., Elder, B.D., Bilz, S., Befroy, D., Romanelli, A.J., and Shulman, G.I. (2004). Mechanism of hepatic insulin resistance in non-alcoholic fatty liver disease. J. Biol Chem. *279*, 32345–32353.

Sörhede Winzell, M., Magnusson, C., and Ahren, B. (2005). The apj receptor is expressed in pancreatic islets and its ligand, apelin, inhibits insulin secretion in mice. Regul. Pept. *131*, 12–17.

Tatemoto, K., Hosoya, M., Habata, Y., Fujii, R., Kakegawa, T., Zou, M.X., Kawamata, Y., Fukusumi, S., Hinuma, S., Kitada, C., et al. (1998). Isolation and characterization of a novel endogenous peptide ligand for the human APJ receptor. Biochem. Biophys. Res. Commun. *251*, 471–476.

Tatemoto, K., Takayama, K., Zou, M.X., Kumaki, I., Zhang, W., Kumano, K., and Fujimiya, M. (2001). The novel peptide apelin lowers blood pressure via a nitric oxide-dependent mechanism. Regul. Pept. *99*, 87–92.

Valle, A., Hoggard, N., Adams, A.C., Roca, P., and Speakman, J.R. (2008). Chronic central administration of apelin-13 over 10 days increases food intake, body weight, locomotor activity and body temperature in C57BL/6 mice. J. Neuroendocrinol. *20*, 79–84.

Zhong, J.C., Yu, X.Y., Huang, Y., Yung, L.M., Lau, C.W., and Lin, S.G. (2007). Apelin modulates aortic vascular tone via endothelial nitric oxide synthase phosphorylation pathway in diabetic mice. Cardiovasc. Res. *74*, 388–395.